PAPER • OPEN ACCESS

Pulsed cooperative backward emissions from non-degenerate atomic transitions in sodium

To cite this article: Jonathan V Thompson *et al* 2014 *New J. Phys.* **16** 103017

View the article online for updates and enhancements.

IOP ebooks™

Bringing you innovative digital publishing with leading voices to create your essential collection of books in STEM research.

Start exploring the collection - download the first chapter of every title for free.

Pulsed cooperative backward emissions from non-degenerate atomic transitions in sodium

Jonathan V Thompson[1], Charles W Ballmann[1], Han Cai[1], Zhenhuan Yi[1], Yuri V Rostovtsev[2], Alexei V Sokolov[1,5], Phillip Hemmer[1], Aleksei M Zheltikov[1,3], Gombojav O Ariunbold[1,4,5] and Marlan O Scully[1,5,6]

[1] Texas A&M University, College Station, TX 77843, USA
[2] University of North Texas, Denton, TX 1155, USA
[3] International Laser Center, M.V. Lomonosov Moscow State University, Moscow, 119992, Russia
[4] National University of Mongolia, Ulaanbaatar, 210646, Mongolia
[5] Baylor University, Waco, TX 76798, USA
[6] Princeton University, Princeton, NJ 08544, USA
E-mail: ariunbold@tamu.edu

Abstract

We study backward cooperative emissions from a dense sodium atomic vapor. Ultrashort pulses produced from a conventional amplified femtosecond laser system with an optical parametric amplifier are used to excite sodium atoms resonantly on the two-photon $3S_{1/2}$–$4S_{1/2}$ transition. Backward superfluorescent emissions (BSFEs), both on the $4S_{1/2}$–$3P_{3/2}$ and $4S_{1/2}$–$3P_{1/2}$ transitions, are observed. The picosecond temporal characteristics of the BSFE are observed using an ultrafast streak camera. The power laws for the dependencies of the average time delay and the intensity of the BSFEs on input power are analyzed in the sense of cooperative emission from nonidentical atomic species. As a result, an absolute (rather than relative) time delay and its fluctuations (free of any possible external noise) are determined experimentally. The possibility of a backward swept-gain superfluorescence as an artificial laser guide star in the sodium layer in the mesosphere is also discussed.

1. Introduction

Species-specific remote sensing/spectroscopy in the sky has been a profound challenge in modern applied physics. The conventional atmospheric light detection and ranging (LIDAR) techniques [1, 2] have essential tools for detecting traces of air impurity at long distances. A tremendous amount of research has been devoted to upgrading conventional LIDAR techniques. Among them, the femtosecond-LIDAR, based on commercially available high-intensity femtosecond (fs) lasers, has been demonstrated [3]. A fs filament formation [4] in air enables propagation of fs pulses for distances of tens of kilometers in scale. In any case, LIDAR techniques rely on incoherent light-scattering processes which are the fundamental limitation for LIDAR's performance. Therefore, an emerging new technology is inevitable.

Recently, coherent standoff spectroscopic (SOS) techniques have been proposed [5, 6]. In particular, one SOS technique [5] is intended to maintain a backward swept-gain for the successive two-photon induced superradiance (SR) [7, 8]/superfluorescence (SF) [9, 10] emissions. In general, in SF or SR, a macroscopic dipole moment of the medium builds up from initially incoherently or coherently excited atomic states. As an extension of the usual SF for two-level atoms, two-photon absorption laser-induced backward SF has recently been observed in cesium [11] and rubidium (Rb) [12, 13]. Coherent temporal control of backward SF in Rb vapor has been studied as an improvement over conventional standoff sensing [13], and high-gain, directional backward superfluorescence emissions have been observed in air [14, 15]. The backward emissions interpreted as 'coherence-brightened laser-like' [15] (via the presence of atomic coherence) and 'laser-like' [14] (via the absence of atomic coherence) are produced from two-photon excited oxygen atoms as a result of the two-photon photolysis of oxygen molecules in ambient air. Numerical simulations [16] in terms of cooperative phenomena (SF, SR, etc) have been performed to elucidate the observed experimental results in [15].

In this work, we study the backward superfluorescent emissions (BSFEs) from two-photon excited sodium (Na) atomic vapor. There are many advantages to working specifically with Na atoms. This two-photon excitation mechanism of Na is similar to that in [14, 15]. However, any relaxations (collisions, dephasings, spontaneous emissions, etc), photolysis, or ionizations are discarded for dense Na vapor. This is because superfluorescent emissions occur for short timescales before other relaxation processes have any effect. It is also clean, in the sense that it involves the ground ($3S_{1/2}$) and the lowest possible two-photon excited ($4S_{1/2}$) states. Since the closely spaced Na D-lines are involved, one should expect double BSFEs that are in the infrared range (around 1140 nm). Conventional spectrometers and ultrafast streak cameras have adequate quantum efficiency in this wavelength range. This is not the case in the Rb atomic system, where the center wavelength of the BSFE is about 5 μm [13]. Moreover, the present research is of great interest from the viewpoint of standoff sensing with SF. The last, but not least, consideration that we mention here is the existence of an atomic layer of Na in the mesosphere. An extensive research effort has recently been dedicated to the practical implementations of an artificial Na laser guide star (LGS) for ground-based telescopes that can improve images distorted due to the atmospheric layer by using adaptive optical techniques
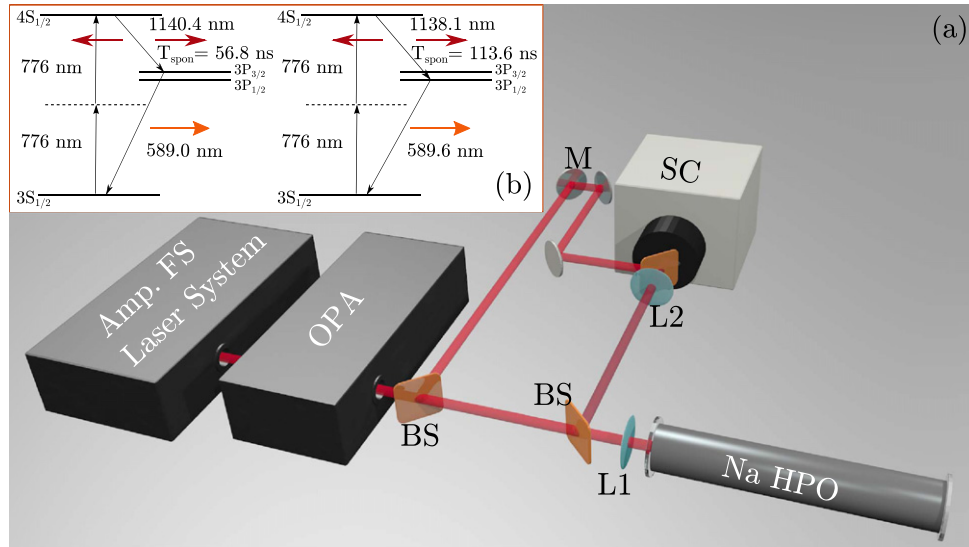
Figure 1. (a) Experimental setup: Amp. FS laser system (a femtosecond amplified laser system); OPA (optical parametric amplifier); BS (beamsplitter); L1,2 (lenses); SC (streak camera) and Na HPO (Na heat pipe oven at 450 °C). (b) The atomic level scheme.

[17]. The conventional approach for LGS is based on resonance fluorescence with the Na D2-line (589 nm) [18–20]. However, there are several fundamental limits [21], including the saturation effect and the limited number of return photons, to name two. To overcome the saturation effect, polychromatic LGS has been extensively studied [18–21]. In spite of some scalability limitations, the present research may have possible applications in polychromatic LGS technology.

The rest of this paper consists of sections dedicated to the experimental setup, observed results, discussion of the results, and conclusions.

2. Experimental setup

In figure 1(a), the experimental setup is sketched. The experimental setup consists of a commercial Ti:sapphire amplified laser system (Coherent, Inc.) with an optical parametric amplifier (OPA, Coherent, Inc. OPerA-VIS/UV), a homemade heatpipe oven containing Na metal (Na HPO), two types of fiber spectrometers (Ocean Optics USB2000+, STellarNet EPP2000-NIR-InGaAs), and a Hamamatsu (C5680 with a minimum resolution of 2 ps) streak camera. From the OPA we obtained 100 fs long pulses, centered at 776 nm with a 20 nm full width at half maximum (FWHM) and up to 17 mW average power at a repetition rate of 1 kHz. The beam size was about 3 mm. A reflective attenuator (not shown in figure 1(a)) was used to control the power of the input beam to the heatpipe oven. The reference 776 nm input pulse shown in figure 1(a) was used to remove laser jitter and obtain relative pulse delay with the streak camera. Its temporal width of about 5 ps also determines the camera resolution obtained in the experiment. Either a 40 or 50 cm focal-length lens was used to focus the input beam into the middle of the heatpipe oven. The properties of the BSFE were qualitatively reproducible for both cases. Therefore, in the following, only the results from the 40 cm lens configuration are
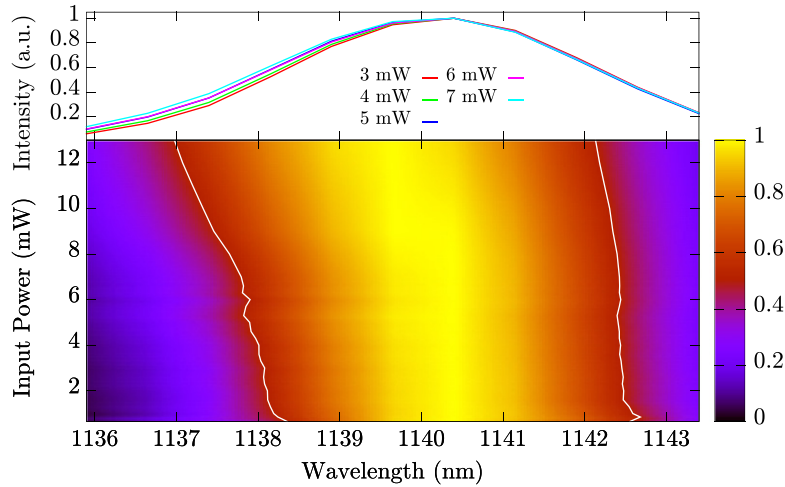
Figure 2. The spectra of BSFEs as functions of input power where the three-dimensional figure in the bottom was interpolated from experimental data.

presented. Fifteen grams of Na were loaded into the center of the pipe at the time of construction [22, 23]. The heatpipe oven has an inner diameter of 2.5 cm, a total length of 61 cm, and tilted windows to avoid reflections. The heated region is about 15 cm long with a density of 1.7×10^{16} atoms per cm^3 at 450 °C and 15 Torr Argon (buffer gas) pressure. A 1 mm microscope glass slide was used as a beam splitter for detection of the backward emissions.

The Na atomic level scheme and two-photon excitation mechanism are shown in figure 1(b). The input 776 nm ultrashort pulses excite the Na atoms via a two-photon process resonant to the $3S_{1/2}$–$4S_{1/2}$ transition. The macroscopic atomic dipole moment can eventually build up to initiate the backward and forward SF emissions at 1140 and 1138 nm (on the $4S_{1/2}$–$3P_{3/2}$ and $4S_{1/2}$-$3P_{1/2}$ transitions, respectively) as well as the forward SF emissions at 589.0 and 589.6 nm (on the $3P_{3/2}$–$3S_{1/2}$ and $3P_{1/2}$–$3S_{1/2}$ transitions, respectively). The forward SF emissions occur simultaneously, and are also referred to as yoked-SF [11]. The generated BSFEs at 1140 and 1138 nm were filtered to eliminate a residual of the 776 nm light by an 830 nm long-pass filter (Semrock, EdgeBasic BLP01–830R-25). To measure the generated forward signals, the microscope glass slides were also used (not shown in figure 1(a)).

3. Observed results

The backward emissions are measured both by spectrometer and streak camera. A simple measurement of the backward emission yields an estimate of the divergence angle to be no larger than 17.5 mrad. The spectra of the backward emitted light were collected by the spectrometer and averaged over 20 samples for different input power.

The normalized spectra are plotted in two different ways in figure 2. Note here that the resolution of the spectrometer (~0.7 nm) is not sufficient to clearly separate the 1140 nm and 1138 nm emission peaks. The edges at the spectral FWHM are plotted by white solid curves. As we see in figure 2, the normalized spectra become broader to the blue-side as power increases. This is because of an increased portion of the 1138 nm spectral component in addition to 1140 nm in the actual measured spectra.
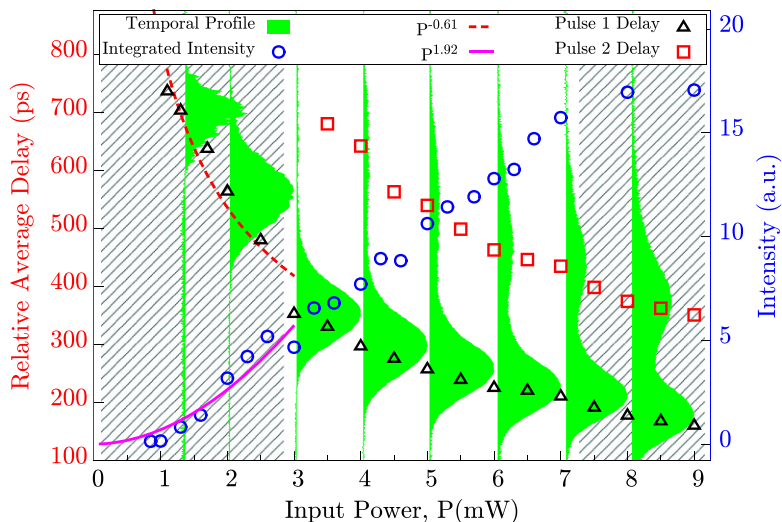
Figure 3. Experimentally observed data. The averaged temporal pulse shapes (in logscale and normalized), relative average time delay, and integrated intensity of the backward emitted light as functions of input power are depicted by the filled green curves, red squares and black triangles, and blue circles, respectively.

The integrated intensity of the backward spectra is plotted as a function of input power as blue circles in figure 3. The nonlinear power dependence of the integrated intensity on input power is demonstrated. Backward emitted light was also focused into the streak camera with a 10 cm lens. Two hundred samples were taken by streak camera for each power setting. Some averaged temporal profiles (filled green curves) of the BSFEs for different input powers are also shown normalized in logscale in figure 3. For low-input power (below 3 mW), only the 1140 nm SF was measured. In this case, the average delay and integrated intensity are fitted with $\sim P^{-1}$ and $\sim P^2$, respectively, where P is the input power. Note that since the threshold power is too small, it is not included here. This type of pure/single SF has already been studied in the literature [11, 13]. However, for input power above 3 mW, picosecond time-resolved double SF pulses were recorded. We identify the second, delayed pulse as a 1138 nm SF pulse, as seen in figure 2. We obtained the average delay of the SF pulses with respect to the incident pump laser (reference) pulse and its dependence on the input laser intensity. The average time-delay of the 1140 nm and 1138 nm SF pulses relative to the reference input pulse are plotted as functions of input power, shown as black triangles and red squares, respectively, in figure 3. Additionally, the forward SF pulses on the upper and lower transitions were also measured for different input powers. The ratio between the forward and backward SF (at about 1140 nm) pulse energies on the upper transitions was about 30. The conversion efficiency of the input 776 nm into the backward emission was 0.0035 %.

4. Discussion

A cooperative emission in two nonidentical atoms has been theoretically studied in [24]. Similarly, cooperative emissions from nondegenerate atomic transitions are sophisticated, and rigorous experimental and theoretical tests are beyond the framework of the present work. Clearly, a simultaneous observation of the double SF pulses in atomic vapor is intriguing in its
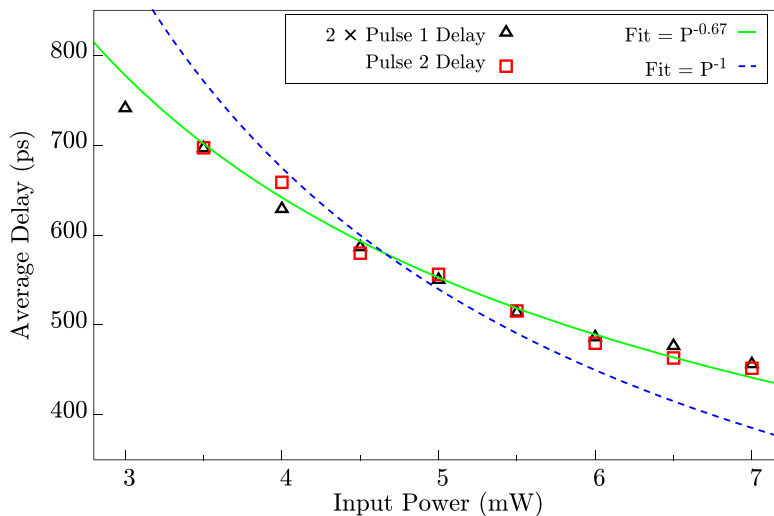
Figure 4. Absolute average time delay of the BSFE with the measurement-related offset removed. The time delay of the 1140 nm BSFE is multiplied by a factor of two to show its relationship with the 1138 nm time delay. The data points are fitted by a power law.

own right. To understand the observed data, we estimate the following. For the sake of simplicity, half of the excited atoms independently emit 1140 nm SF pulses, and the other half emit 1138 nm SF pulses. An SF scaling parameter, $\tau_R \sim T_{spon}/N$, and an initial (tipping) angle are the only parameters necessary to fully determine the whole SF process [10], where T_{spon} and N are the spontaneous lifetime and number of excited atoms, respectively.

We observe that the spontaneous lifetime, T_{spon}, for the $4S_{1/2}$–$3P_{3/2}$ transition (56.8 ns) is two times faster than that for the $4S_{1/2}$-$3P_{1/2}$ transition (113.6 ns). Consequently, the 1138 nm SF pulse is delayed by two times more than the 1140 nm SF pulse. From this simple statement, one can find an offset between the relative and absolute time-delay for each power. This is a complicated task to determine experimentally. Our analysis is for the unshaded region in figure 3, (i.e., the interval between 3 to 7 mW input power). The offset corrected data for this region are shown in figure 4, where the offset was about 17 ps and depended very little on input power. The data were fitted with power laws. As a result, the SF delay is approximately proportional to the inverse of the input power. Note that for two-photon excitation, the number of excited atoms is proportional to the square of the input power. Therefore, this is quantitative evidence that each of the backward 1140 nm and 1138 nm emissions is independently governed by the laws of oscillatory SF phenomena. Similar (single, but not double) oscillatory SF in Rb vapor was reported in our earlier work [25].

Naively, one would expect that starting from the same excited level, $4S_{1/2}$, to two states, $3P_{1/2}$ and $3P_{3/2}$, the SF would go via the channel with larger coupling to electromagnetic radiation, similar to mode competition in laser physics [27]. In figure 3, we actually observe two SF pulses. Their relative intensities depend on the level of pump intensity, but the delay times for both SF pulses are different by a factor of 2. This is related to the different electric dipole moments for these transitions because the delay time is inversely proportional to the spontaneous emission rate, γ. For these two transitions, the spontaneous lifetime and cooperative frequencies differ by this same factor of 2. Indeed, the SF pulse (Rabi frequency) starts as $\Omega_{SF} \propto \sqrt{D\gamma/t}\ I_1(2\sqrt{2D\gamma t})$, and the delay time, $t_{delay} \simeq 1/(D\gamma)$,
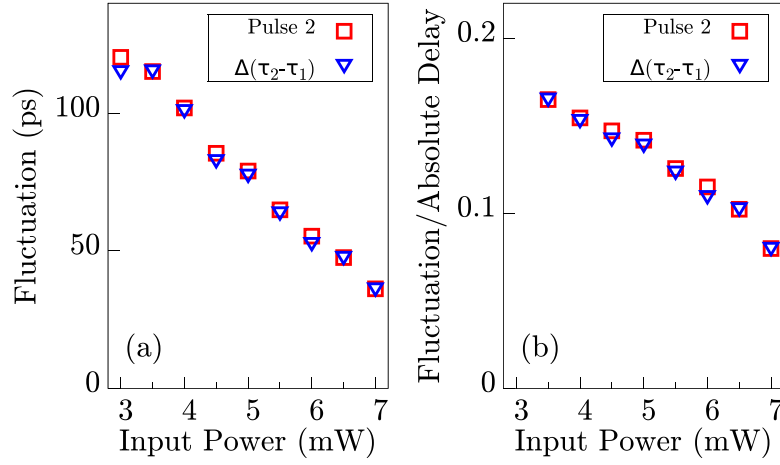
Figure 5. (a) Root-mean-square fluctuations $\left(\sqrt{\langle(\Delta\tau_i)^2\rangle}\right)$ in time delay of the 1138 nm SF pulses as a function of input power. (b) The ratio of the fluctuations and average time delay $\left(\sqrt{\langle(\Delta\tau_i)^2\rangle}\Big/\langle\tau_i\rangle\right)$ versus input power.

where $D = 3\lambda^2 Nz/(8\pi)$, I_1, t, z, and λ are the linear optical density, first-order Bessel function, time, pulse propagation distance, and SF center wavelength, respectively. Because the delays of the SF pulses are different by a factor 2 (the ratio of the spontaneous emission rates), they do not overlap in space, and the coherence between the $3P_{1/2}$ and $3P_{3/2}$ states does not play any role.

Based on the simplified theoretical estimations, we find the total number of excited atoms, N, to be 10^{10} and the τ_R for the 1140 nm SF pulse to be $\tau_R \approx 20$ ps at an input power of 2 mW. As expected, the two sets of time-delay data for the 1140 nm and 1138 nm SF pulses coincide by a factor of two, as shown in figure 4. Due to a high gain factor used when recording data with the streak camera, the temporal shape of the 1140 nm pulse might be distorted compared to the 1138 nm pulse. We obtained the width of the 1138 nm SF pulse for different input powers and compared it to the average time delay. The 1138 nm pulse width is inversely proportional to input power.

We also attained the time delay fluctuations for each backward SF pulse separately via the formula $\sqrt{\langle(\Delta\tau_i)^2\rangle} = \sqrt{\langle\tau_i^2\rangle - \langle\tau_i\rangle^2}$, where τ_i is the time delay of a single BSFE relative to the laser reference pulse, as captured by the streak camera. Additionally, histograms for the statistical distribution as in [28] were constructed. The fluctuation of the 1138 nm SF as a function of input power is shown in figure 5(a). The time-delay fluctuations decrease as input power increases. The quantum fluctuations in alkali vapor were measured in [26, 28]. The fluctuations of the difference between the two pulses were also obtained and shown in figure 5. This difference removes the nonreproducible extrinsic fluctuations (e.g., the laser pulse shot to shot noise) [28]. The power dependence of the ratio between the fluctuations and average time delay is shown in figure 5(b). It is interesting to point out that this ratio for the 1138 nm SF pulses clearly demonstrates an inverse dependence on input power, as is expected. A quantum theory predicts this ratio for SF from N two-level atoms to be proportional to $1/\ln(N)$ [29].

The present study of backward emissions from Na is important for laser guide star (LGS) technology. Although several worldwide large telescopes already operate with LGS, the number

of return photons is fundamentally limited [18]. To overcome these specific limitations, so-called polychromatic LGS has emerged [19]. The concept of polychromatic LGS is to utilize either single-photon (at 330 nm [20]) or nondegenerate two-photon (at 569 and 589 nm [21] or at 1140 and 589 nm [18]) excitations of Na atoms and detect cascade fluorescence at different wavelengths, including 589 nm. In particular, the pulsed bichromatic LGS scheme proposed in [18] uses nondegenerate two-photon excitation, whereas a resonant degenerate two-photon excitation is used in the present work. In [18] they estimated that for their bichromatic LGS scheme, about 50 photons (25 times above the detection limit) can be collected in a solid angle of $\sim 10^{-9}$ steradian (sr) from the 4π sr-radiated fluorescence from $\sim 10^{12}$ excited atoms in the sodium layer of the mesosphere. The tendency of directionality of BSFE increases the number of return photons in the same solid angle (10^{-9} sr). A simple estimation has been given in our previous work [13], where it is estimated that a 100 J laser pulse directed into the mesosphere would return a photon flux of 10^{8} per second, per square centimeter. We estimate there to be hundreds of return photons.

5. Conclusion

In conclusion, we observed backward cooperative emissions from nonidentical Na atomic species. Temporally well-separated, nondegenerate double superfluorescence pulses were measured. The average time delay and its fluctuations of the measured superfluorescence pulses are determined with minimum possible systematic/experimental errors.

The present excitation scheme, which could be applied as a type of polychromatic laser guide star, has several advantages over conventional, monochromatic laser guide star. For instance, the fundamental problems of saturation (less than 50% of the atomic population can be transferred to the excited state via one-photon processes) and differential tilt (refraction due to the atmosphere) can be solved using the present two-photon excitation scheme with or without involving cooperative phenomena where nearly 100% population excitation can be achieved; differential tilt can be corrected with a polychromatic (double superfluorescence pulses) return signal. Although only about four sodium atoms per mm^3 exist in the mesosphere, a 10 km-thick layer could still validate cooperative effects via e.g., gain sweeping and provide for a better collimation in the backward direction, thus increasing the number of return photons. A rigorous numerical simulation for both fluorescence (the same as in [18]) and superfluorescence (together with an implementation of the backward swept-gain technique [5]) from the Na layer utilizing the present two-photon excitation mechanism will be given elsewhere.

Acknowledgements

References

[1]　Steinbrecht V, Rothe K W and Walther H 1989 *Appl. Opt.* **28** 3616

[2]　Bisson S E, Goldsmith J E M and Mitchell M G 1999 *Appl. Opt.* **38** 1841

[3]　Kasparian1 J *et al* 2003 *Science* **301** 61

[4]　Couairon A and Mysyrowicz A 2007 *Phys. Rep.* **441** 47

[5]　Kocharovsky V, Cameron S, Lehmann K, Lucht R, Miles R, Rostovtsev Y, Warren W, Welch G R and Scully M O 2005 *Proc. Natl Acad. Sci. USA* **102** 7806

[6]　Hemmer P R, Miles R B, Polynkin P, Siebert T, Sokolov A V, Sprangle P and Scully M O 2011 *Proc. Natl Acad. Sci. USA* **108** 3130

[7]　Dicke R H 1954 *Phys. Rev.* **93** 99

[8]　Rehler N E and Eberly J H 1971 *Phys. Rev.* A **3** 1735

[9]　Bonifacio R and Lugiato L 1975 *Phys. Rev.* A **11** 1507

[10]　MacGillivray J C and Feld M S 1976 *Phys. Rev.* A **14** 1169

[11]　Brownell J H, Lu X and Hartmann S R 1995 *Phys. Rev. Lett.* **75** 3265

[12]　Lvovsky A I 1998 *PhD Thesis* Columbia University (http://people.ucalgary.ca/~lvov/thesis-complete.pdf)

[13]　Ariunbold G O, Sautenkov V A, Rostovtsev Yu V and Scully M O 2014 *Appl. Phys. Lett.* **104** 021114

[14]　Dogariu A, Michael J B, Scully M O and Miles R B 2011 *Science* **331** 442

[15]　Traverso A J *et al* 2012 *Proc. Natl Acad. Sci. USA* **109** 15185

[16]　Yuan L, Hokr B H, Traverso A J, Voronine D V, Rostovtsev Yu, Sokolov A V and Scully M O 2013 *Phys. Rev.* A **87** 023826

[17]　Ageorges N and Dainty C 2000 *Laser Guide Star Adaptive Optics for Astronomy* (Dordrecht: Kluwer)

[18]　Biegert J and Diels J-C 2003 *Phys. Rev.* A **67** 043403

[19]　Foy R *et al* 2007 *Proc. SPIE* **6691** 66910R

[20]　Pique J-P, Moldovan I C and Fesquet V 2006 *JOSAA* **23** 2817

[21]　de Chatellus H G, Pique J-P and Moldovan I C 2008 *JOSAA* **25** 400

[22]　Hite D, Deebel M, Thoreson E, Lengacher C, Miers R E and Masters M F 1997 *Am. J. Phys.* **65** 1017

[23]　Grove T T, Hockensmith W A, Cheviron N, Grieser W, Dill R and Masters M F 2009 *Eur. J. Phys.* **30** 1229

[24]　Ficek Z, Tanas R and Keilich S 1986 *Optica Acta* **33** 1149

[25]　Ariunbold G O, Kash M M, Sautenkov V A, Li H, Rostovtsev Yu V, Welch G R and Scully M O 2010 *Phys. Rev.* A **82** 043421

[26]　Vrehen Q H F and der Weduwe J J 1981 *Phys. Rev.* A **24** 2857

[27]　Sargent M III, Scully M O and Lamb W E 1974 *Laser Physics* (Reading MA: Addison-Wesley)

[28]　Ariunbold G O, Sautenkov V V and Scully M O 2012 *Phys. Lett.* A **376** 335

[29]　DeGiorgia V 1971 *Opt. Commun.* **2** 362